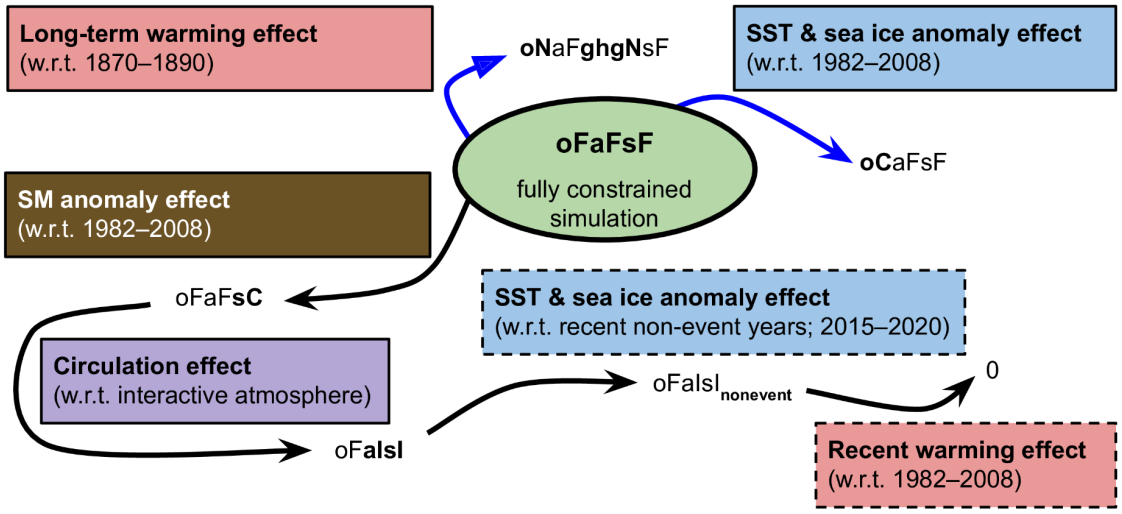

Fig. 1: Disentangling framework to estimate physical drivers of the heat wave. Black arrows denote contributions that are part of the additive disentangling framework presented by Wehrli et al. (2019), and indicate the pathway used to estimate the contributions of dynamic and thermodynamic drivers. For example, we start with the fully constrained simulation (oFaFsF) and compare it to a simulation with climatological soil moisture (oFaFsC); their temperature anomaly difference indicates the effect of anomalous soil moisture. Next, by comparing the simulation with climatological soil moisture to the ensemble mean of simulations where winds are calculated interactively, we obtain the circulation effect, and so on. Note that contributions estimated based solely on simulations with interactive atmosphere are considered to be 'generic' estimates (dashed border), contrary to 'event-specific' effects estimated with a constrained atmosphere (toward actual winds according to ERA5). All these heatwave contributions are displayed for the 2021 PNW event in **Fig. 2c**. Blue arrows indicate additional estimates of 'event-specific' ocean and long-term warming effects that are not part of the original additive framework.

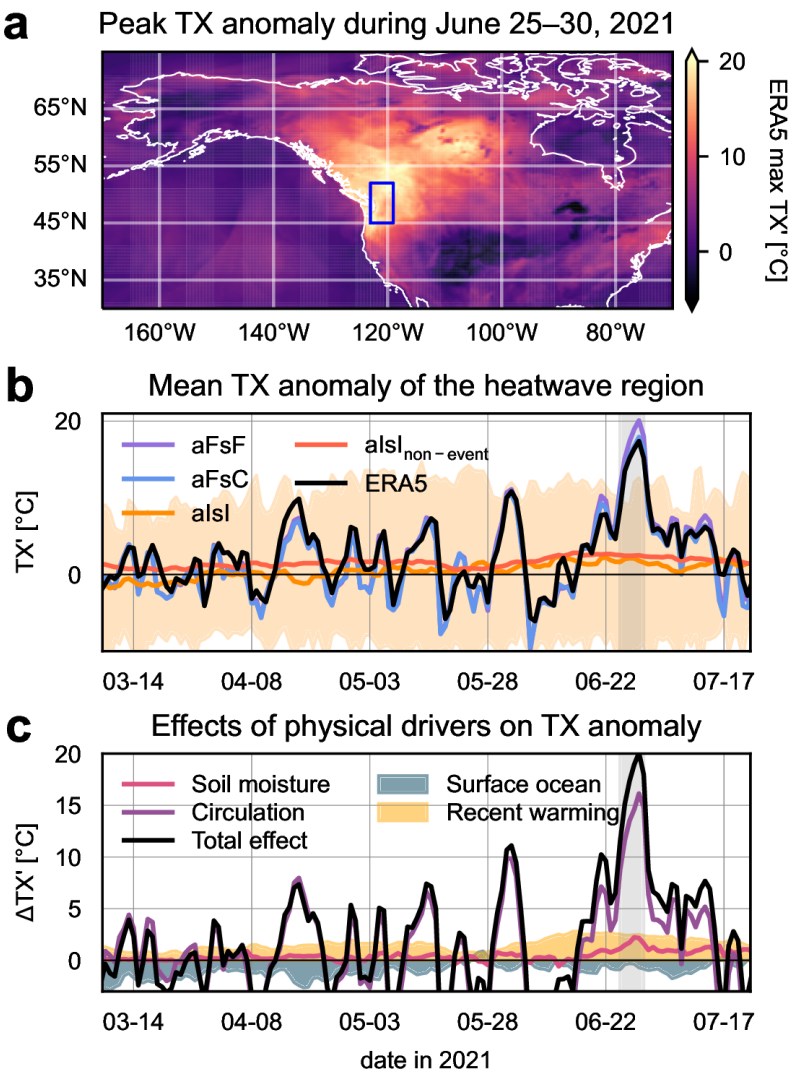

Fig. 2: Unprecedented temperature anomalies in late June 2021 in the Pacific Northwest. (a) Highest daily maximum temperature anomaly reached in ERA5 from June 25 to 30, 2021. During these last days of June, the event reached its peak intensity in the heatwave region used throughout this study (blue contour). Anomalies are calculated with respect to 1982–2008. **(b)** Anomaly timeseries for the heatwave region, depicting area-weighted mean daily maximum temperatures from ERA5 (black line). In addition, multiple simulations from CESM are shown: the 'reference' — fully constrained atmosphere and soil moisture (aFsF; purple), same but with constrained climatological soil moisture (aFsC; blue), and interactive atmosphere and soil moisture (aIsI; orange). The latter consists of 80 simulations, whose ensemble mean is indicated by a solid line, while the shading visualizes minima and maxima. The ensemble mean of aIsI simulations for recent non-event years (2015–2020) is also shown. **(c)** Physical drivers in the additive disentangling framework (**Fig. 1**), obtained by TX' differences visualized in (b). The sum of these contributions is equal to TX' indicated by the fully constrained simulation.

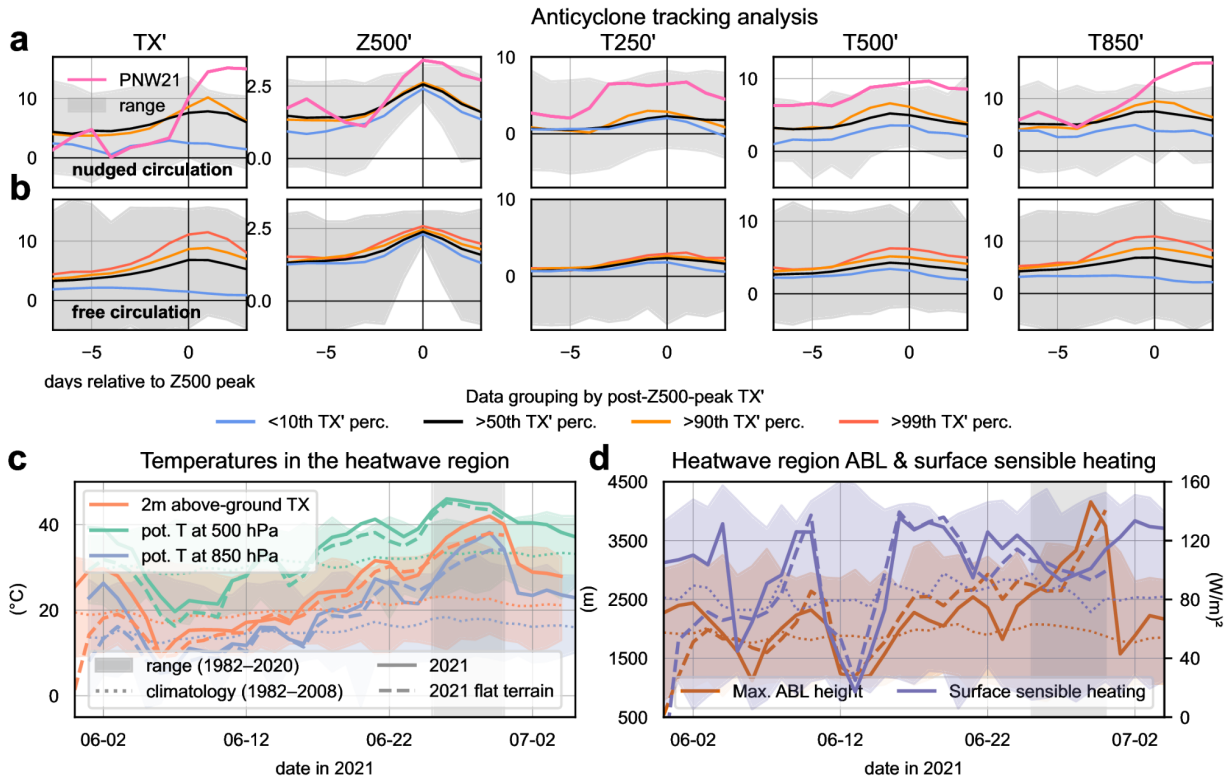

Fig. 3: Investigating the dynamics of the 2021 PNW heatwave with CESM. **(a)** Results for nudged atmospheric circulation, with near-surface temperature anomalies, Z500 anomalies, and temperature anomalies in the upper, middle and lower troposphere (from left to right). All data are based on a 10°x10° domain centered on the respective anticyclone position and are plotted with respect to the day of peak Z500 intensity. A range excluding the PNW 2021 event (pink line) indicates previous minima and maxima. In addition, events are grouped based on their near-surface heat anomaly, or more specifically, several TX' percentiles (10^{th}, 50^{th}, 90^{th}) after the Z500 peak. **(b)** As (a), but based on simulations with interactive atmosphere and soil moisture. The 99^{th} TX' percentile group is visualized along with the same data groups already employed for (a). **(c)** Temperatures in the heatwave region close to the surface, and the potential temperatures at 850 and 500 hPa (defined here as the temperature that air would have if brought adiabatically to 2m above ground), from the base CESM simulation with nudged winds. Data are presented for the actual 2021 event (solid lines), as a range for previous years since 1982, and as the climatological mean (dotted lines). Temperatures for an otherwise identical simulation with flat terrain in western North America are also indicated (dashed lines). **(d)** As (c), but showing the daily maximum ABL height and mean surface sensible heat flux instead.

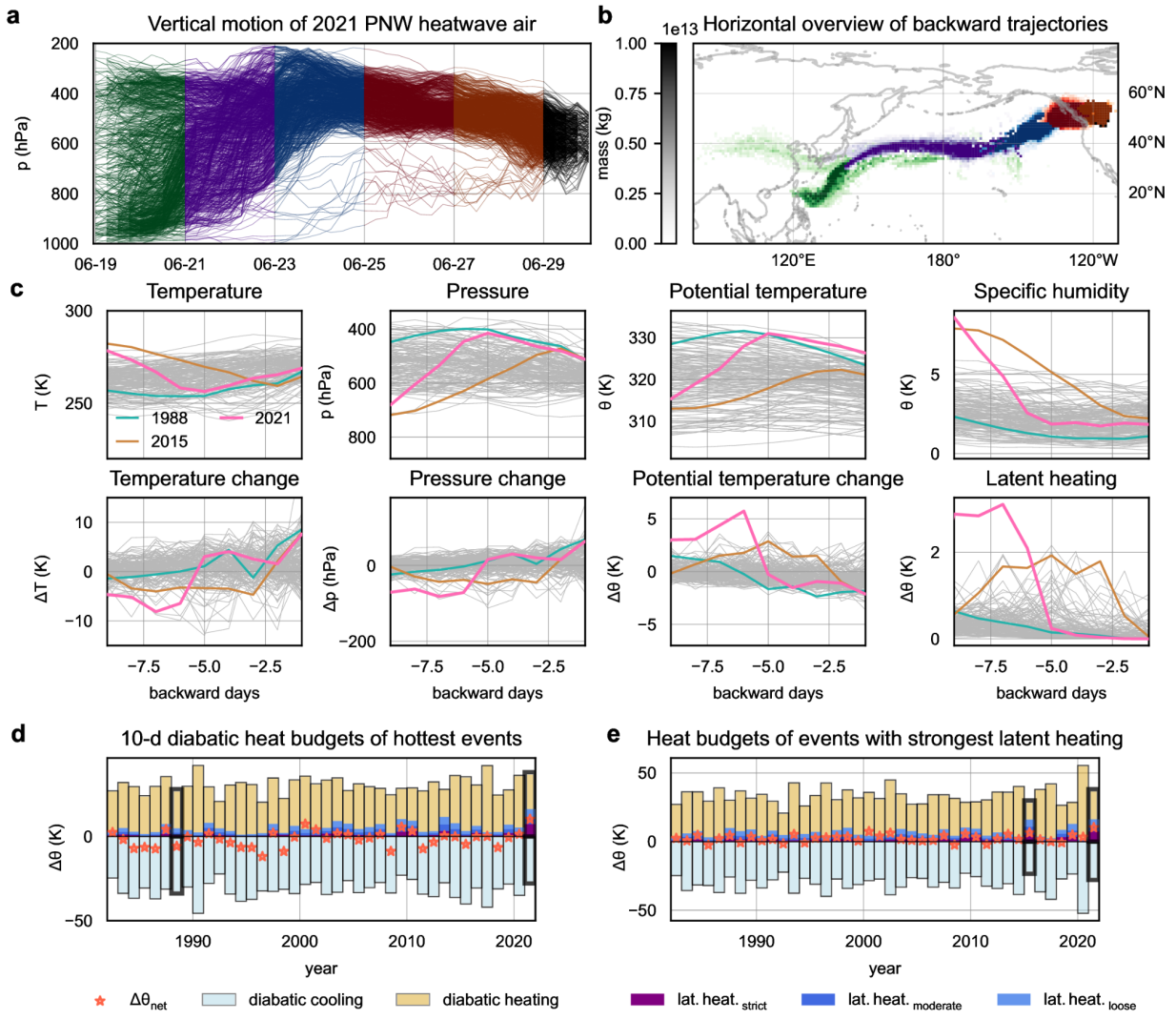

Fig. 4: Backward trajectory analysis of the PNW 2021 heatwave and other North American hot events. (a) Vertical backward analysis of air residing over the heatwave region in late June 2021, with colors marking different time periods. For aesthetic reasons, only 1000 randomly selected trajectories are shown. **(b)** Horizontal overview of backward trajectories, expressed as gridded air mass and colored consistently with the time dimension in (a). **(c)** Evolution of temperature, pressure, potential temperature and specific humidity for the air involved in North American hot events (gray lines in the upper row), averaged over all respective backward trajectories. The 2021 PNW heatwave (red), as well as events in 1988 (orange) and 2015 (green) are emphasized (thick lines with markers). The lower row displays temporal changes of the same variables as displayed above. **(d)** Trajectory-averaged diabatic heating budgets of the most intense hot extreme for every summer since 1982. In addition to diabatic heating, cooling and the resulting net change in potential temperature (w.r.t. backward day -10), estimates of latent heating for 3 sets of criteria (see Methods) are depicted. The 1988 and 2021 PNW heatwaves are highlighted (thick black edges). **(e)** Like (d), but showing the hot event with strongest upwind latent heating for each year. The 2015 and 2021 PNW events are highlighted.

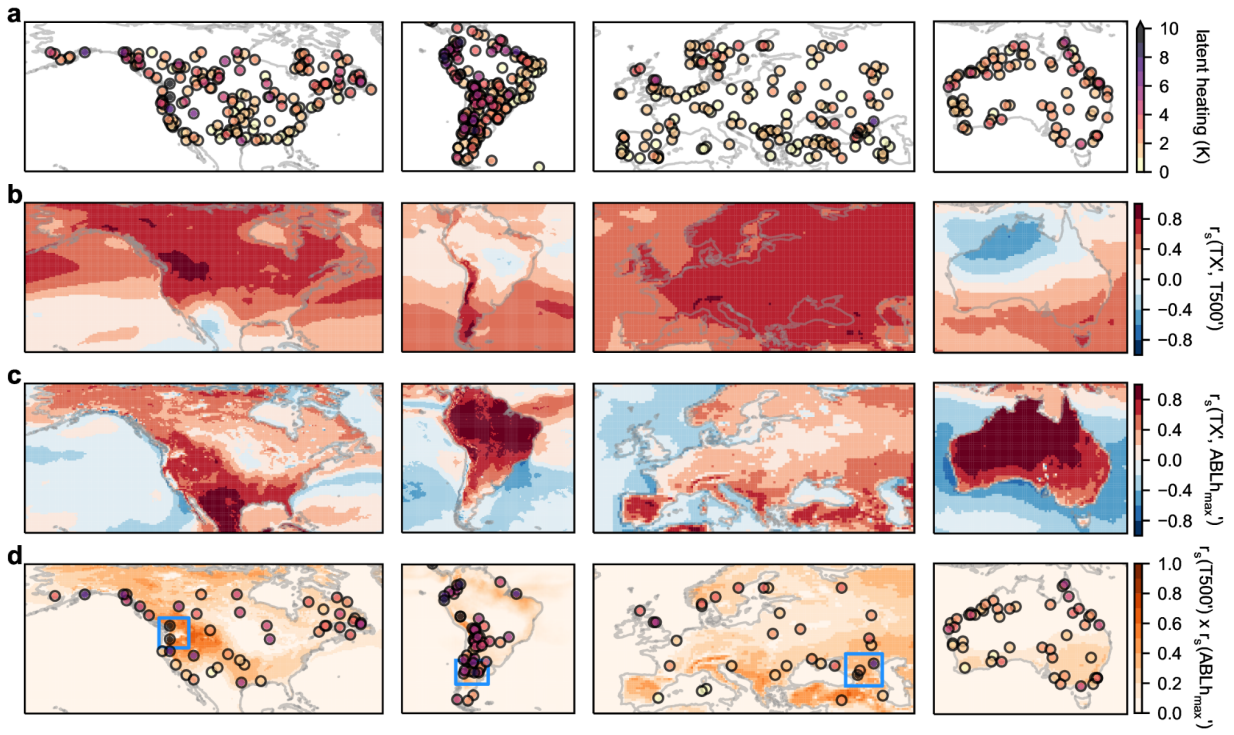

Fig. 5: Upwind latent heating prior to downwind heatwaves. (a) Upwind latent heating of summer heatwaves from 1982 to 2021 for North and South America, Europe and Australia, determined with TRACMASS–ERA5. **(b)** Correlation coefficients of ERA5 daily maximum near-surface and mean 500-hPa temperature anomalies; based on JJA for North America and Europe, and DJF for South America and Australia, 1982–2021. **(c)** As (b), but for the correlation of near-surface maximum temperature and maximum ABL depth. **(d)** Upwind latent heating of air masses from (a) that experience net diabatic heating in the 10 days prior to arrival over the respective heatwave region. The orange shading visualizes the product of (b) and (c), and indicates regions where hot summer days are frequently accompanied by anomalously deep ABLs and above-normal 500-hPa temperatures. The highlighted areas (PNW, Pampas, North Caucasus) are potentially favorable for the occurrence of heatwaves with a similar anatomy as the 2021 PNW event.